

DRL-Based QoS-Aware Resource Allocation Scheme for Coexistence of Licensed and Unlicensed Users in LTE and Beyond

Mahdi Nouri Boroujerdi*, Mohammad Akbari[†], Roghayeh Joda[†], Mohammad Ali
Maddah-Ali*, Babak Hossein Khalaj*

*Department of Electrical Engineering, Sharif University of Technology, Tehran,
Iran

Email: {ma.nouri, maddah_ali, khalaj}@sharif.edu

[†]Department of Communication Technologies, ICT Research Center (ITRC),
Tehran, Iran

Email: {m.akbari, r.joda}@itrc.ac.ir

Abstract

In this paper, we employ deep reinforcement learning to develop a novel radio resource allocation and packet scheduling scheme for different Quality of Service (QoS) requirements applicable to LTE-advanced and 5G networks. In addition, regarding the scarcity of spectrum in below 6 GHz bands, the proposed algorithm dynamically allocates the resource blocks (RBs) to licensed users in a way to mostly preserve the continuity of unallocated RBs. This would improve the efficiency of communication among the unlicensed entities by increasing the chance of uninterrupted communication and reducing the load of coordination overheads. The optimization problem is formulated as a Markov Decision Process (MDP), observing the entire queue of the demands, where failing to meet QoS constraints penalizes the goal with a multiplicative factor. Furthermore, a notion of continuity for unallocated resources is taken into account as an additive term in the objective function. Considering the variations in both channel coefficients and users' requests, we utilize a deep reinforcement learning algorithm as an online and numerically efficient approach to solve the MDP. Numerical results show that the proposed method achieves higher average spectral efficiency, while considering delay budget and packet loss ratio, compared to the conventional greedy min-delay and max-throughput schemes, in which a fixed part of the spectrum is forced to be vacant for unlicensed entities.

Index Terms

Deep reinforcement learning, spectrum sharing, radio resource management, QoS requirement, machine learning.

I. INTRODUCTION

With rapidly growing demand for mobile wide-band radio access, developing bandwidth-efficient strategies has the highest importance. Allowing different operators to share the same bandwidth, Dynamic Spectrum Sharing (DSS) is known as one of the most promising 5G enablers, alleviating the lack of spectral efficiency [1]. LTE-Unlicensed (LTE-U) is a good example of spectrum sharing, where the main idea is to offload a fraction of LTE traffic to unlicensed bands in order to increase the overall throughput of a typical LTE system, while minimizing the degradation in performance of WiFi users [2, 3].

On the other hand, efficient resource allocation and packet scheduling scheme is a keystone in designing a bandwidth-efficient strategy. Classic resource allocation and packet scheduling schemes in LTE are based on simple heuristics such as round robin scheduling or equal throughput for all users in the network. More advanced schemes include some sort of feedback from the user side as well, such as channel coefficients, to optimize a predefined metric, e.g. maximizing the throughput. Another group also takes some users' Quality of Service (QoS) parameters into account [4]. Being simple and quite inefficient, efforts have been made to propose more advanced schemes [5, 6]. These works, however, provide the solution only for a fixed set of system's parameters, including channel coefficients, and need to resolve the optimization problem whenever these parameters change, which incurs a huge and repetitive computation burden.

As both DSS and resource allocation deal with a dynamic problem, due to changes in channel coefficients, number of users, request profiles, etc., plenty of works focused on the use of Reinforcement Learning (RL), a suitable framework to use when complex decisions need to be made on a regular basis, to solve such problems [7–9]. Early works on use of RL for resource allocation, such as [10], have applied lookup table based RL, where a simple RL-based technique is proposed to allocate resources based on a combined metric of spectral efficiency, average delay and packet loss ratio in an LTE network. In more complex settings, lookup table approach may not be practical, as saving Q values for a big state-action space requires a very large memory, in addition to taking very long time for the agent to be trained.

Introducing neural networks in RL context, also known as Deep Reinforcement Learning (DRL),

was a huge leap toward solving this problem [11]. In [12], DRL is applied to allocate radio and core resources in a network slicing scenario, where a weighted sum of spectral efficiency and required Quality of Experience (QoE) by each slice is maximized. For this goal, a Long Short Term Memory (LSTM) is used to predict traffic of each slice and allocate the resources to the slices accordingly. However, since resources are allocated to slices based on the traffic prediction model, there might be some deviation from real demands, and inefficiency in resource allocation. In addition, channel states are not taken into account in the resource allocation strategy. In [13], a heterogeneous network scenario is considered where picocells and femtocells provide area coverage cooperatively, while user association and resource allocation is solved jointly with a DRL approach. Each user chooses among the available set of BSs and for the selected BS among the available channels. In [13], QoS is defined only as a function of the minimum Signal to Interference plus Noise Ratio (SINR) constraint, without considering latency. The coexistence of WiFi and LTE-U is explored in [14], where LSTM is used to predict the traffic pattern of WiFi users in the unlicensed bands. Then, some of the delay-tolerant requests in LTE are served in time-windows predicted to be occupied with lower likelihood. The LTE small Base Stations (BSs) use RL to allocate the resources such that long-term air time fairness is guaranteed for BSs and WiFi access points.

On the other hand, some standards allow unlicensed users to use licensed spectrum, in case they have a sharing agreement with the original license-holder, and are also equipped with Cognitive Radios (CRs), to communicate in the licensed LTE bands [15]. Note that, typically, unlicensed users need to release the resources as soon as they are being used by the licensed ones. In a network with active licensed users, this can significantly increase the signaling overhead among unlicensed users or even make the resources useless when they are sparse in time and frequency. To resolve this challenge, in this paper we propose an alternative approach, in which the BS tries its best to help unlicensed users by leaving the longest sequence of consecutive resource blocks, in time and on the same frequency, unoccupied, provided that the required QoS for licensed users are guaranteed. This would allow an unlicensed user to use a sub-channel for communication with minimum interruption from the BS, and with minimum overhead for coordination.

The proposed scheme relies on DRL to efficiently assign radio frequency resources to the requests demanded by the licensed users, while no assumption is made about any prior knowledge of the requests' distributions. In fact, the main goal of the proposed scheme is to keep some resources

unallocated (free) for the unlicensed users such that there is a higher probability that the free resources belong to the same frequency slot at successive continuous time slots. As we assume no cooperation among the licensed and the unlicensed users, such approach eases the search process of unlicensed users as they do not need to make a full sweep over the entire frequency band to find vacancies at every time slot. In addition, the overhead of handshaking signaling between the unlicensed communicating entities is reduced¹. As RL intrinsically learns by interacting with the environment, the agent chooses a policy, acts accordingly, observes the result, and modifies its policy for the next steps. This is in contrast with the traditional approaches, which require to solve the optimization problem once in a while. Our results show that the proposed scheme is able to maximize the average spectral efficiency, satisfy the required QoS of the received requests, and simultaneously set aside a continuous spectrum for the unlicensed users. As we do not assume any coordination among licensed and unlicensed users, the proposed method can be categorized among the non-cooperative spectrum allocation methods [1]. Furthermore, no limitation is imposed on the unlicensed users. As a result, any already-developed scheme in CR network context can be utilized by unlicensed users. It is worthwhile to mention that in this paper, LTE is only used as a typical implementation model for the physical and access layer, and the proposed method is equally applicable to other schemes that use CQI tables, such as 5G New Radio (NR), as well [16].

The contributions of this paper are summarized as follows

- We formulate the optimization problem for allocating time-frequency resources to the incoming requests, constrained by QoS of the users' requests in terms of latency and a notion of continuity of unallocated resources to be utilized by the unlicensed users. This can be considered as a decentralized resource sharing for the unlicensed users as we do not assume any coordination among the BS and the unlicensed users, nor do we assume any knowledge of the unlicensed users' channel states by the BS.
- We formulate the problem as a Markov Decision Process (MDP), where by defining the mathematical representation of the states, action and the optimization problem, we apply model-free deep RL to solve it. The requests are generated from a set of stationary, but unknown to the BS, distributions.

¹Such handshakings are necessary prior to settle a communication between a sender and a receiver including the agreement over the new frequency band.

- We use experience replay and double Q networks, two famous techniques known to be efficient in deep RL, to improve the convergence of the deep RL algorithm.
- We assume general time-variant frequency selective channels among the BS and the User Equipments (UEs). The optimization process specifies the resource blocks associated with the requests at every step of the RL agent. This is more general than many previous papers which only determined the fraction of the allocated bandwidth for a specific user or a slice, e.g. [12].

The rest of the paper is organized as follows. Section II describes the system model. Mathematical formulation of the problem of interest is given in Section III. Section IV provides a brief review of RL, and how it can be combined with the idea of neural networks to arrive at a deep RL scheme. The process of learning with RL is described in Section V. Numerical results along with the discussion are given in Section VI. The paper is concluded in Section VIII.

II. SYSTEM MODEL

We consider a cellular network where a number of users are served by a BS at the downlink side. The channel access method is considered to be Orthogonal Frequency Division Multiple Access (OFDMA), hence each user is assigned a set of time-frequency resources during its service time. Each user's request is sent by its UE to the BS as a tuple including its required service type, with some predefined parameters, and its quantized channel estimate. Requests arrive continuously to the BS over time. We assume that the arrival process of the requests is quasi-stationary² and the BS is unaware of the distribution of the arrival process.

The BS is responsible for allocating time-frequency resources to the requests sent by the users. The resources consist of some time-frequency blocks called Resource Blocks (RBs). Each RB has T [s] time-width and W [Hz] frequency-width. The BS places the incoming request(s) into a buffer with fixed length L , as long as it has vacancy and drops the request(s) otherwise. It performs resource allocation by assigning all the RBs belonging to the current time step to some of the requests in the requests' buffer. The time steps are referred to as $\{n\}_1^N$ and are the smallest BS time units. The requests in the buffer are indexed as $j \in \{1, 2, \dots, L\}$. The BS is given a total of R RBs in a given time step. At each time step, we allocate the RBs to the

²It simply requires the requests' distributions to stay the same long enough so that the learning algorithm is able to track the changes in the distribution. As we will see in Section VI, the proposed scheme converges in almost several tens of thousands of iterations, which translates into almost 10 to 20 seconds of requests' observation.

available requests in the requests' buffer for the current time step and then proceed to a new one. Hence, we ignore the time index and refer to each of the RBs of the current time step by only the frequency index k , where $k \in \{1, 2, \dots, R\}$. Finally, we define another set of indices, called the RL steps, as follows. Consider N time steps including NR RBs. We index these RBs as $\{0, 1, 2, \dots, NR - 1\}$, calling each one as an RL step, such that RL step i refers to RB index $k = i \bmod R + 1$ at time step $n = \lfloor \frac{i}{R} \rfloor + 1$, where $\lfloor \cdot \rfloor$ indicates the floor function³.

A. Channel Model

In general, the channel between the BS and each user is a time-frequency varying channel. However, we assume the channel is constant in each RB. Let's denote the channel vector from the BS to the user corresponding to the j th request in the requests' buffer at time n over R RBs with $\mathbf{h}^j[n] = [h_1^j[n], h_2^j[n], \dots, h_R^j[n]]^T$, where $h_k^j[n] \in \mathbb{C}, \forall k \in \{1, 2, \dots, R\}$. We assume a one-to-one correspondence between the set of users and the set of requests. In other words, every new request is issued by a user, which potentially has a new channel state. In general, there might be many requests issued by the same user. As we will see in Section VI, almost all of the incoming requests are accepted by the BS. Hence, this assumption does not affect the performance of the resource allocation, since the spectral efficiency results are averaged over the entire simulation time. Taking such correspondence into account, we will use the words *user* and *request* interchangeably in the text. Let's also assume that the k th RB is assigned to the j th request at time n . The signal received by the user corresponding to the j th request can then be written as

$$y^j[n] = h_k^j[n]x^j[n] + z^j[n], \quad (1)$$

where $x^j[n]$ is the transmitted symbol and $z^j[n]$ is the additive Gaussian noise. We assume that the users experience a mixture of small-scale and large-scale fading, hence the channel coefficient $h_k^j[n]$ can be written as $h_k^j[n] = \sqrt{l^j} \zeta_k^j[n]$, where l^j and $\zeta_k^j[n]$ denote the large scale and small scale fading, respectively. Large scale fading coefficient for a specific requests is assumed to stay constant as long as that request is being served and hence is not a function of n , while small-scale fading coefficients change after every coherence period, denoted by τ [s]. As can be seen, for a single request j , small scale fading coefficient $\zeta_k^j[n]$ also depends on the RB index

³The name RL step refers to each step RL agent takes while interacting with the environment. The reason this name is chosen will become more clear in Section V.

k , while large scale fading coefficient l^j are the same for all RB indices. We assume that the j th UE has always access to a perfect estimate of its channel vector $\mathbf{h}^j[n]$. By using (1), the instantaneous SINR observed by the j th user at the k th RB and at time step n can be written as⁴

$$\text{SINR}_k^j[n] = \frac{\mathbb{E} |x^j[n]|^2 |h_k^j[n]|^2}{\mathbb{E} |z^j[n]|^2} = \frac{P_t |h_k^j[n]|^2}{R \sigma_n^2}, \quad (2)$$

where P_t is the BS's total transmit power, and σ_n^2 is the noise power at the UE's terminal. It is assumed that the BS is using uniform power allocation for all RBs. As channel estimate vector $\mathbf{h}^j[n]$ is valid for a period of length τ , we know that $\text{SINR}_k^j[n]$ remains constant during a coherence period. We assume that each UE calculates the CQI as a function of the measured SINR, and reports it to the BS as a ϕ -bit integer. Each CQI corresponds to a predefined Modulation and Coding Scheme (MCS), as in LTE standard [17]. We assume that the CQI values are available at the BS for all the users corresponding to the requests in the BS's requests' buffer and for all the RBs at any time step⁵. We denote the CQI values for the j th user by the vector $\mathbf{c}^j[n] = [c_1^j[n], c_2^j[n], \dots, c_R^j[n]]$, where the index n is used to note that this estimate is updated just at the beginning of every coherence time and hence, is in general time-dependent⁶. Next, we define a mapping used by the BS to find the Spectral Efficiency (SE) corresponding to each CQI value.

Definition 1 (CQI-SE Mapping). *CQI-SE mapping $\mathcal{T} : [0, 2^{\phi-1}] \rightarrow \mathbb{R}$ is defined as a fixed mapping, where $\mathcal{T}[m], \forall m \in [0, 2^{\phi-1}]$, as a function of CQI, denotes the instantaneous (per RB) achievable spectral efficiency by the user to which the RB is assigned.*

Using Definition 1, the BS is able to calculate the number of deliverable bits for the j th request in the requests' buffer at RB k at time n as

$$t_k^j[n] = WT \mathcal{T}[c_k^j[n]] \quad (3)$$

⁴Without loss of generality, we assume that the interference received from the neighboring BSs are negligible. As long as there is no cooperation among the neighboring BSs, the given argument can be extended to a multicell scenario by considering interference as noise.

⁵In general, depending on the patterns and the number of subcarriers given to the BS, there might be some sort of correlation among different components of the channel vector for each UE. This can be utilized by the UE to perform some sort of compression to return these values to the BS in an efficient manner.

⁶More precisely, $\mathbf{c}^j[n/\tau]$ denotes the channel vector for each coherence period.

We assume that the number of bits calculated in (3) is fully deliverable to the j th user. In other words, $\mathcal{T}[c_k^j[n]]$ is below the capacity of its corresponding channel.

B. Requests' Buffer

As previously mentioned, each request received by the BS includes two entries: First, its service type and second, the CQI of its corresponding user. Service type is defined as follows.

Definition 2 (Service Types). *A service type m , $m \in \{1, 2, \dots, \theta\}$, for some integer θ , is defined by a tuple (u_1^m, u_2^m) , where u_1^m specifies the number of bits to be delivered for service type m and u_2^m refers to the maximum tolerable latency (in terms of the number of time steps) for the delivery of u_1^m bits⁷.*

As soon as the BS receives a single incoming request, it puts the request into the requests' buffer. The buffer's length L is a fixed design parameter. As soon as the buffer becomes full, the incoming requests are dropped until at least a request is either satisfied or missed as per the following definitions. A request is said to be *missed* if it has not received sufficient resources within its tolerable latency and said to be *satisfied* otherwise.

Let us now give a more detailed description of the requests' buffer. The j th element of the requests' buffer at RL step i , denoted by $\mathbf{q}^j[i]$, is a vector of size $R + 3$. The 1st element $q_1^j[i]$ denotes the request's service type index which remains fixed as long as the j th request stays in the buffer. The 2nd element $q_2^j[i]$ denotes the remaining time up to the end of which the j th request is valid, called Time To Live (TTL) here for simplicity, it starts from a predefined value, $u_2^{q_1^j[i]}$, and is decremented at every single time step, i.e. $q_2^j[n + 1] = q_2^j[n] - 1$, where $n = \lfloor \frac{i}{R} \rfloor + 1$. The variable $q_2^j[n]$ is always non-negative. As soon as it becomes zero, the request is missed and removed from the buffer. The 3rd element $q_3^j[i]$ denotes the number of required bits by the j th request that has not been delivered so far. It starts from a predefined value, i.e. $u_1^{q_1^j[i]}$, and is decremented every time the j th request is given some resources. The remaining R elements $[q_4^j[i], q_5^j[i], \dots, q_{R+3}^j[i]]^T$ specify the number of deliverable bits by the RBs for the j th request, which can be written as $\mathbf{t}^j[i] = [q_4^j[i], q_5^j[i], \dots, q_{R+3}^j[i]]^T$ using (3), and are updated at

⁷ A typical service a user requests, such as video streaming or file download consists of many units of fixed/variable sizes that should be delivered to the user uninterruptedly. We assume that the requests for each data unit is received by the BS separately, hence the BS only observes the arrival process of the requests for such data units.

the beginning of every new coherence time. Now, we are ready to give a more formal definition of the requests' buffer:

Definition 3 (Requests' Buffer). *The requests' buffer at RL step i , is defined as*

$$\mathcal{B}[i] = \{\mathbf{q}^j[i] | j \in \{1, 2, \dots, L\}\}. \quad (4)$$

It should be noted that initially, the requests' buffer is empty, i.e. $\mathcal{B}[0] = \{\mathbf{q}^j[0] = \mathbf{0} | j \in \{1, 2, \dots, L\}\}$. As the requests arrive, the buffer is filled with the incoming requests. As we will see, the order by which a request is pushed in or popped out of the buffer depends on the resource allocation scheme and is not known in advance, hence the buffer is neither a FIFO nor a LIFO buffer.

C. Continuity Vector

As mentioned earlier, our objective is to propose a scheme which allocates the resources to the licensed users efficiently, and also keeps the continuity of the unallocated resources for the unlicensed users. First, let us define the concept of *continuity vector*.

Definition 4 (Continuity Vector). *The continuity vector at time step n is defined as $\mathbf{v}[n] = [v_1[n], v_2[n], \dots, v_R[n]]^T$, where $v_k[n]$ denotes the number of last continuous unallocated resources, from the n th time step backward in time and including the n th time step, at RB index k for $k \in \{1, 2, \dots, R\}$.*

As an example, a snapshot of the allocated and unallocated RBs for the last four time steps is given in Fig. 1. The continuity vector for this figure at the last time step, i.e. n , is given as $\mathbf{v}[n] = [1, 1, \dots, 2]^T$, where $v_1[n] = 1$ means, for the current time step, the first RB is unallocated, but the first RB at the previous time step is occupied. Likewise, $v_R[n] = 2$ means that the R th RB is unallocated for the current time step and for the previous time step as well. Next, we define the *continuity function*

Definition 5 (Continuity Function). *The continuity function with respect to the parameter $C \in \mathbb{N}$ is defined as*

$$g_C^k[n] = \begin{cases} 1 & \text{if } v_k[n] \geq C \\ 0 & \text{O.W.} \end{cases}, \quad (5)$$

where $v_k[n]$ is the k th element of the continuity vector given in Definition 4 and C is a fixed integer called the *continuity length*.

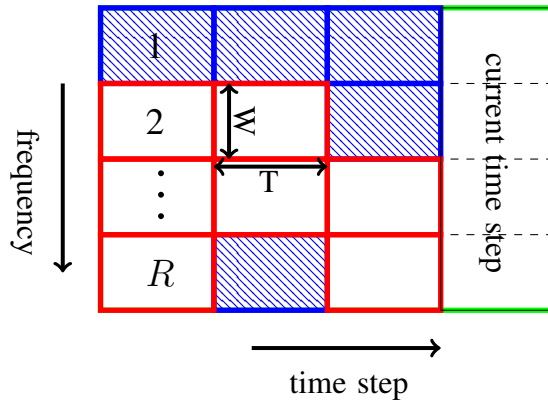


Fig. 1. An illustration of the continuity vector $\mathbf{v}[n] = [1, 1, \dots, 2]^T$ based on Definition 4 for an example snapshot consisting of the last four time steps. The hatched and the free rectangles refer to the allocated and unallocated RBs respectively. The numbers inside rectangles refer to the RB index at each time step.

The continuity function is simply a step function with the value of 1 for RB index k if the number of last successive unallocated resources are at least equal to C and with the value of 0 otherwise.

III. PROBLEM FORMULATION

A. Markov Decision Process (MDP)

Markov Decision Process (MDP) provides the mathematical tool to formalize a decision making problem with known dynamics. An MDP is defined as a tuple $\langle \mathcal{S}, \mathcal{A}, \mathcal{P}, \mathcal{R}, \gamma \rangle$, where \mathcal{S} represents the state space, \mathcal{A} represents the action space, \mathcal{P} represents the transition probabilities, \mathcal{R} represents the rewards and γ is the discount factor [18].

In order to formulate the optimization problem in an MDP form, we need to define the *state* first. The state should be defined in such a way that grasps the whole dynamics of the system, which include the adding/dropping of the requests in the buffer, the changes in the channel coefficients of the users demanding the requests, the continuity measure of the unallocated resources and the current RB index. Using the definitions given in Section II, we can define the *state* as follows.

Definition 6 (State). The state $\mathbf{s}_i \in \mathcal{S}$ is defined as

$$\mathbf{s}_i = [\mathbf{b}[i]^T, \mathbf{v}[n]^T, \psi]^T, \quad (6)$$

where $\mathbf{b}[i]$ is the requests' buffer $\mathcal{B}[i]$ written in the vector form as $\mathbf{b}[i] = [\mathbf{q}^1[i]^T, \mathbf{q}^2[i]^T, \dots, \mathbf{q}^L[i]^T]^T$,

$\mathbf{v}[n]$ is the continuity vector as defined before and $\psi \in \{1, 2, \dots, R\}$ is the current RB index as $\psi = i \bmod R + 1$.

Remark 1. The state \mathbf{s} , defined in Definition 6, has the dimension $(R + 3) \times L + R + 1$ which grows linearly with the buffer length L and also with the number of available resource blocks R .

Remark 2. Some parts of the state \mathbf{s} defined in Definition 6 can change only after a time step n , while other parts can change after every RL step i . The former includes $\mathbf{v}[\cdot]$, $q_2^j[\cdot]$, and the latter includes ψ , $q_1^j[\cdot]$, $q_3^j[\cdot]$. The vector $\mathbf{t}^j[\cdot]$ can change only after several time steps corresponding to a coherence period.

Remark 3. Based on Definition 6, the number of delivered bits for a specific request j so far at RL step i , can be written as $u_1^{q_1^j[i]} - q_3^j[i]$.

The next important step to define an MDP, is the action.

Definition 7 (Action). The action is defined as $a_i \in \mathcal{A} = \{0, 1, 2, \dots, L\}$, where $a_i = 0$ means to leave the current RB unallocated (free), and $a_i > 0$ means to allocate the current RB to the $j = a_i$ th request in the requests' buffer.

Remark 4. For any action $a_i > 0$, $a_i \in \mathcal{A}$, taken from state $\mathbf{s}_i \in \mathcal{S}$, there is a possibility that action a_i refers to an empty space inside the requests' buffer. This can happen in the case where there are less requests than the value of action a_i in the buffer at state \mathbf{s}_i . This action is called an invalid action and as a result, the corresponding RB is left unallocated.

B. Problem Formulation

The next concept we need to define before arriving at the mathematical formulation for the optimization problem is the concept of *spectral efficiency*. As we have already assumed, the CQI is available at the BS and hence, the spectral efficiency for each state is the number of deliverable bits in that state divided by the allocated bandwidth, as given in the following definition.

Definition 8 (Spectral Efficiency). Spectral efficiency for each RB is defined as the number of deliverable bits in that RB, divided by the product of the time-width and frequency-width of a single RB, i.e. $W \times T$.

As we will see later in Section V, the resource allocation procedure is such that a state-action pair (\mathbf{s}_i, a_i) specifies the assignment of a single RB to a specific request. This notion of spectral efficiency can be calculated using the following remark.

Remark 5 (Spectral Efficiency). *Spectral efficiency, as a function of the state \mathbf{s}_i and the action a_i can be calculated as*

$$SE(\mathbf{s}_i, a_i) = \begin{cases} \frac{q_{\psi+3}^{a_i}[i]}{WT} & \text{if } a_i > 0 \\ 0 & \text{if } a_i = 0 \end{cases}, \quad (7)$$

where ψ and $q_{\psi+3}^{a_i}[i]$ are both parts of the state \mathbf{s} according to Definition 6.

For the case where $a_i = 0$, no request is selected and the RB is left free, hence we should have $SE = 0$. This can be seen from (7) as well.

For any other case, i.e. $a_i > 0$, a request is chosen from the requests' buffer by the action a_i as the buffer index. The selected request should be $\mathbf{q}^{a_i}[i]$ according to Definition 3. The vector $\mathbf{t}^{a_i}[i]$ which refers to the last R components of $\mathbf{q}^{a_i}[i]$ contains the number of deliverable bits for every RB for the selected request. Finally, the current RB index ψ corresponds to the $\psi + 3$ th component of the request $\mathbf{q}^{a_i}[i]$. Based on the discussion given in Section II-B, this component can be written as $q_{\psi+3}^{a_i}[i]$.

Remark 6. *The notion of Spectral Efficiency defined in (5) is in fact an optimistic metric. This is the case since the requests to which resources are allocated currently might be missed in the future. This should be taken into account and will be handled shortly.*

Now, we formulate an optimization problem which aims to simultaneously maximize the average spectral efficiency, for the delivered requests, keep some RBs unallocated for unlicensed users in a continuous manner as defined in Definition 5, and minimize the number of missed requests. First, we need to quantify the sum of spectral efficiencies for a single time step n . This can be written as

$$\sum_{\lfloor \frac{i}{R} \rfloor + 1 = n} SE(\mathbf{s}_i, a_i) - \frac{\zeta[n]}{WT}, \quad (8)$$

where $\zeta[n]$ denotes the number of allocated bits corresponding to the requests that are missed at time n . The first term in (8) is simply a sum over the spectral efficiencies for different RBs belonging to the n th time step based on Remark 5 and the second term refers to the share of missed requests at time n that has previously been taken into account in the spectral

efficiency of previous time steps and must be deducted from it. The variable $\zeta[n]$ can be written as $\zeta[n] = \sum_{m \in \mathcal{Z}(\tilde{s})} \left(u_1^{q_1^m[i]} - q_3^m[i] \right)$ where \tilde{s} can be any state from the set $\tilde{s} = \{s_i | \lfloor \frac{i}{R} \rfloor + 1 = n\}$ ⁸ and $\mathcal{Z}(\tilde{s})$ is the set of all missed requests in the requests' buffer at state \tilde{s} . Next, we take into account the effect of continuity for the n th time step. Using Definition 5, this can be written as

$$\sum_{k=1}^R g_C^k[n]. \quad (9)$$

Finally, we need to take into account the effect of latency. This can be written using the concept of TTL defined earlier. We set this term such that its value approaches zero in the case where the request with the minimum latency is about to be missed, i.e. its TTL is close to zero. This can be written as

$$1 - \exp \left(-\delta \min_{l \in \mathcal{Y}[n]} \left(\frac{q_2^l[n]}{u_2^{q_1^l[n]}} \right) \right), \quad (10)$$

where $\mathcal{Y}[n]$ refers to the set of nonempty requests in the requests' buffer at time n and δ is a parameter which controls how fast or how slow (10) moves towards zero. The TTL values are normalized to the maximum possible TTL value of each service type to make sure that the scheme is fair across different service types. Now, we are ready to combine (8), (9) and (10) to formulate the optimization problem as follows

$$\begin{aligned} & \max_{\{a_i\}_{i=0}^{NR-1}} \limsup_{N \rightarrow \infty} \frac{1}{N} \sum_{n=1}^N \left\{ \left[\alpha \sum_{\lfloor \frac{i}{R} \rfloor + 1 = n} \left(\text{SE}(s_i, a_i) - \frac{1}{RWT} \sum_{m \in \mathcal{Z}(s_i)} \left(u_1^{q_1^m[i]} - q_3^m[i] \right) \right) + \beta \sum_{k=1}^R g_C^k[n] \right] \right. \\ & \left. \times \left[1 - \exp \left(-\delta \min_{l \in \mathcal{Y}[n]} \left(\frac{q_2^l[n]}{u_2^{q_1^l[n]}} \right) \right) \right] \right\}, \quad (11) \end{aligned}$$

where $\limsup(\cdot)$ refers to the supremum limit. As the objective function in (11) is always non-negative and bounded, $\limsup(\cdot)$ is used to make sure potential oscillating solutions to (11) are also included. The objective function in (11) consists of a sum, over N time steps, of three terms where the third one is multiplied by the linear combination of the other two. As the minimum normalized TTL value approaches 0, the third term goes to zero, based on the value of the parameter δ , resulting in the share of the entire n th term to be 0. This serves as a maximum tolerable latency constraint.⁹ The three terms in (11) all depend on the sequence of

⁸This is due to the fact that as soon as some requests are missed at time step n , they are known as missed requests at every state in that time step.

⁹We have tested several other forms for the objective function including the form of three additive terms. Finally, it became clear that the case with the best answers in RL formulation was the one given here, i.e. a linear combination of the first and second terms multiplied by the third term where the third term is in an exponential form.

actions $\{a_i\}_{i=0}^{NR-1}$. Solving (11) at one shot is not possible, since the allocation needs to be done online. The solution should be provided for every time step n as time goes on. Even for a limited value of $N > 1$, there is no causal one shot solution to (11). Apart from the causality issue, the objective function in (11) consists of a Nonlinear Integer Programming. Also, as N grows larger, the dimension of the problem grows as large. Thus, this problem cannot be solved using common optimization frameworks. The online solution, however, can be found by formulating the problem into an MDP form and solving it using RL, which will be discussed in detail in the next two sections.

IV. DEEP REINFORCEMENT LEARNING

A. Introduction to RL

As stated earlier in Section III, MDP formalizes a decision making problem with known dynamics. Based on Definitions 6 and 7, it can be seen that as soon as any action $a_i \in \mathcal{A}$ is taken from the state $s_i \in \mathcal{S}$, the state changes to s_{i+1} , since any new action results in a change in ψ and hence s_i . The state also changes at the beginning of every new time step due to the reduction in the requests' TTL values and at every new coherence time due to change in CQI values. It also changes as soon as a new request arrives, provided that the buffer has vacancy. In summary, the state s_i is seen to be a sufficient statistic for the next state s_{i+1} . So, the problem of resource allocation in (11) can be modeled using an MDP. We are not going to calculate the probabilities for the mentioned transitions of the states, as we will exploit model-free RL which relies on samples and not on the model.

The agent, which interacts with the environments, at every step $i \geq 1$ starts from a state s_i and takes an action a_i , receives an immediate reward r_i and lands in a new state s_{i+1} [19]. As mentioned in Section II, we differentiate between the time step referring to the time each RB spans, which was previously indexed by n , and the RL step which is indexed by i . More clearly, each time step consists of exactly R , RL steps. This difference is important, since the resource allocation, as will be explained in Section V, is done based on the latter .

Before moving on, let us briefly explain the concept of *episode*. Episodes are the subsequences that the agent-environment interaction is broken into. Each episode ends in a state called the *terminal state* [18]. A very well-known example of episodic environment is observed in classic games such as chess where an episode terminates as soon as the game is either won or lost . As we will see in Section VI, the RL agent is trained in an episodic setting.

B. Q Learning with Function Approximation

In order to make proper decisions, the agent needs to have a criterion for the goodness of each state-action pair which is quantified using *action-value function*. Typically, the value function for state-action pair (s_i, a_i) is denoted by $Q(s_i, a_i)$ stored in a table. In complex settings where tabular approach cannot hold all state-action value pairs, due to large memory requirement or very long exploration time, neural networks can be used to represent state-action pairs. Such approach is well supported by the fact that neural networks are universal function approximators [20, 21]. Q function in this case is written as $Q(s_i, a_i, \mathbf{w})$, where \mathbf{w} denotes the weights of the neural network. In this case, weights at step i are updated such that the following mean-squared error is minimized:

$$L_i(\mathbf{w}_i) = \mathbb{E}_{s_i, a_i, r_i} \left[\left(\mathbb{E}_{s_{i+1}} [y | s_i, a_i] - Q(s_i, a_i, \mathbf{w}_i) \right)^2 \right], \quad (12)$$

where $y_i = r_i + \gamma \max_a Q(s_{i+1}, a, \mathbf{w}_i^-)$ is the target, \mathbf{w}_i refers to the weights at iteration i and \mathbf{w}_i^- refers to the weights at some previous iteration. The well known Q learning weights update rule can be derived by differentiating (12) with respect to the weights \mathbf{w}_i , replacing the expectation with single samples and updating the weights every step, $\mathbf{w}_i^- = \mathbf{w}_{i-1}$, as follows [22]

$$\mathbf{w}_i = \mathbf{w}_{i-1} + \kappa \left(r_i + \gamma \max_a Q(s_{i+1}, a, \mathbf{w}_{i-1}) - Q(s_i, a_i, \mathbf{w}_i) \right) \nabla_{\mathbf{w}_i} Q(s_i, a_i, \mathbf{w}_i), \quad (13)$$

where κ is the learning rate and $\nabla_{\mathbf{w}_i}(\cdot)$ denotes differentiation with respect to \mathbf{w}_i . This simple rule is data inefficient, since we use each state-action pairs only once, and more importantly, might result in instability. We will shortly review two famous methods that are used to stabilize the updates and improve the convergence behavior of deep RL.

C. Experience Replay

Inspired by [22], sequences of the observed state, action, reward and next state are stored in a memory called the *replay memory* as $\{\mathbf{s}_i, a_i, r_i, \mathbf{s}_{i+1}, \nu_i\}$, where ν_i is a binary variable indicating whether the next state is a terminal state, $\nu_i = \text{True}$ or not, $\nu_i = \text{False}$. During training, minibatch of size M is taken randomly from the replay memory every time the network is trained. This has the benefit of decorrelating the sequences of observations and actions. In other words, the network is trained with states and actions belonging to different points on the time line and thus, improve the convergence behavior of the neural network.

D. Target Network

Another useful method to stabilize neural network in RL is to use a separate network, called the *target network*, for generating the targets for the weights update in (13). The second network's weights are updated less frequently, at a frequency of N_t in terms of the number of RL steps, compared to the main network. During the interval of each two successive updates of the main network, the target network's weights are kept fixed [22]. So, the target in this case will be

$$y_i = r_i + \gamma \max_a \hat{Q}(s_{i+1}, a, \mathbf{w}_i^-) \quad (14)$$

where \mathbf{w}_i^- and $\hat{Q}(s_{i+1}, a, \mathbf{w}_i^-)$ refer to the weights and the output of the target network, respectively.

We finalize this section by discussing the strategy used to take the actions.

E. ϵ -greedy Strategy

A known issue in RL is *exploration-exploitation dilemma*, which can be simply explained as follows. How should we make a balance between exploring new actions from the known states, which might end up in new unexplored states, and exploiting the best known actions. ϵ -greedy strategy is a common strategy which targets this dilemma. It simply starts from a random action selection strategy and gradually decreases the randomness and instead, increases the chance of

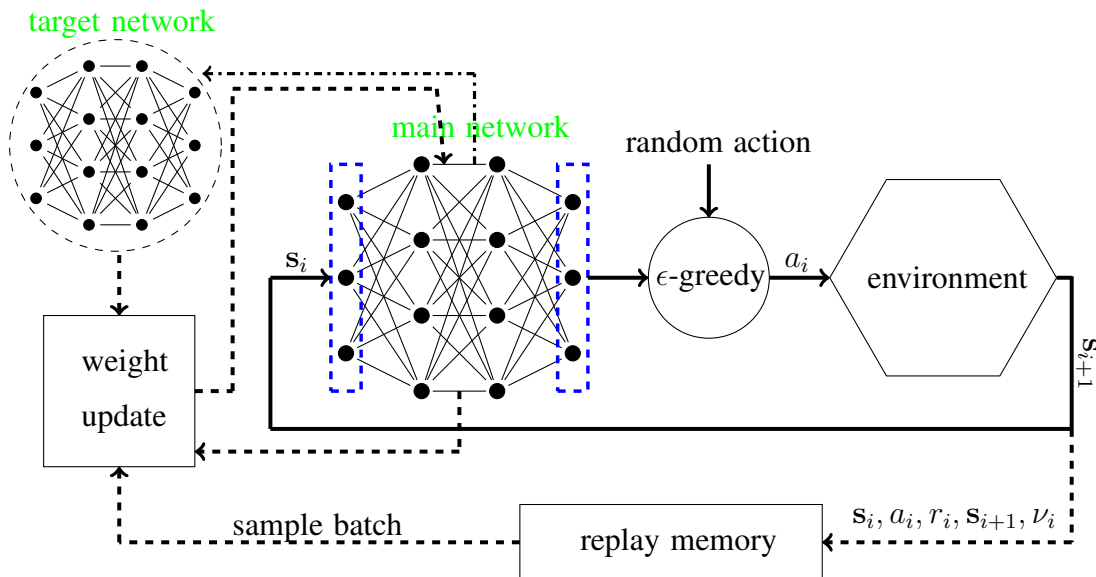


Fig. 2. An illustration of the deep RL mechanism using experience replay and target network to make the network more stable

selecting the best known action for each state.

In this paper, the two ideas that have just been explained, namely the Experience Replay and the Target Network, along with the ϵ -greedy strategy are used. The detailed algorithm is given in Alg. 2. Also an illustration of the deep RL mechanism is depicted in Fig. 2. The only remaining issue will be the rewarding mechanism which is discussed in the next section.

V. RL FRAMEWORK FOR RESOURCE ALLOCATION

In this section, the remaining elements that let one solve (11) in an RL framework are given. The resource allocation scheme is as follows. The agent moves along the two dimensions of frequency and time and allocates the resources in a repetitive procedure. At RL step i , the agent is given an action a_i , which is the output of the ϵ -greedy strategy. If the action is a zero action, i.e. $a_i = 0$, the $k = i \bmod R + 1$ th RB is left unallocated. Otherwise, the action is used as an index and the k th RB is allocated to the $j = a_i$ th request. There is a special case where the action is invalid, meaning that a_i refers to an empty space in the requests' buffer. In this case, the RB is left unallocated as well. The difference with the $a_i = 0$ case is then about the reward given to the agent in these two cases. Once the action is taken by the agent, the state s is updated and fed back to the neural network as input. This process goes on as long as the resource allocation is required.

A. Rewarding Mechanism

What really matters in directing the RL agent towards obtaining the objective in (11) is the rewarding mechanism which is given in Alg. 1. Except for the special cases, i.e. empty buffer and invalid action, the reward consists of three terms in accordance with (11). There are, however, some differences with (11). The first one is the removal of the share in spectral efficiency due to missed requests in the rewarding mechanism. Its role, however, is still being played by the third term in (11) which tries to keep missed requests as low as possible. In case a request is missed, the removed part of the first term approaches 0, and in fact they both act in the same way. The second difference is the normalization of $SE(s, a)$ to its maximum possible value in Alg. 1 in calculating r^1 . This lets α, β have a more balanced effect and hence, facilitates their fine adjustment. Moreover, we accumulate the rewards corresponding to the first and the second terms for different RBs at each time step. At the end of the time step, the accumulated first and second terms form a weighted sum and the result is multiplied by the third term which is given

as the reward to the agent. The reason for delaying the reward up to the end of the time step is that the first and the second terms cannot be nonzero simultaneously. This can lead the agent towards a dominating policy, where only one of the first or the second terms dominates.

We finish this section with a small note. As previously noted in Section IV, each time step consists of R RL steps. The framework could have been designed in a way that all RBs at a time step are allocated at once. This, however, would require a neural network with the output size of R times as large which takes many more iterations to be trained¹⁰. Based on the rewarding mechanism described in this section and the deep RL mechanism described in Section IV, we are ready to describe the resource allocation scheme detailed in Alg. 2.

VI. SIMULATION RESULTS

In this section, the details of the parameters used in the simulations are given. Then, the results are presented and discussed.

A. Parameters of the Channel Model

Based on the discussion given in Section II, the channel vector from the BS to the user corresponding to the j th request in the requests' buffer is denoted by $\mathbf{h}^j[n]$. This is modeled as

$$\mathbf{h}^j[n] = [h_1^j[n], h_2^j[n], \dots, h_R^j[n]]^T = \sqrt{l^j}[\zeta_1^j[n], \zeta_2^j[n], \dots, \zeta_R^j[n]]^T = \sqrt{l^j}\mathbf{\Phi}^{1/2}\mathbf{z}^j[n], \quad (15)$$

where l^j denotes the large scale fading coefficient, $\mathbf{\Phi}$ is the covariance matrix of $\zeta^j[n] = [\zeta_1^j[n], \zeta_2^j[n], \dots, \zeta_R^j[n]]^T$ with the entries given as $[\mathbf{\Phi}]_{m,l} = \omega^{|m-l|}$ for some correlation parameter $\omega \in [0, 1]$ and $\mathbf{z}^j[n] \sim \mathcal{CN}(0, \mathbf{I}_R)$. Large scale fading coefficient l^j is assumed to be constant as long as the j th request is in the requests' buffer and is also equal for all different RBs. $\mathbf{z}^j[n]$ is re-sampled once every coherence period to emphasize that the small scale fading coefficient vector $\zeta^j[n]$ remains unchanged throughout each coherence period and changes independently from one coherence period to another. Large scale fading coefficient and correlation parameter ω are chosen based on Table I [23]. As can be seen from Table I, users are assumed to be uniformly distributed at a distance between 10 and 100 meters from the BS, which operates with a transmit power of 100 mW [24]. Coherence time for small scale fading coefficients is taken to be 12 ms¹¹. White noise is considered on each RB with a bandwidth equal to that of

¹⁰This is in case one-hot encoding is used as the output coding for the neural network.

¹¹Corresponding to a user with a velocity of 10 m/s with the approximate formula $\frac{0.4}{v/c \times f_c}$ for the coherence time [25].

Algorithm 1 Rewarding mechanism for the proposed deep RL Algorithm (at time step $n = \lfloor \frac{i}{R} \rfloor + 1$)

```

1: Input:  $\mathbf{s}_i, a_i$ , Output:  $r_i$ ;  $k = i \bmod R + 1 \in \{1, 2, \dots, R\}$ 
2: Initialize  $r^1 = r^2 = r^3 = 0$ 
3: for  $k \in \{1, 2, \dots, R\}$  do
4:   if the requests' buffer is empty then
5:     return 0
6:   else
7:     if  $a_i$  is an invalid action then
8:       return -1
9:     else
10:       $r^1+ = \text{SE}(\mathbf{s}_i, a_i) / \text{SE}_{\max}, r^2+ = g_C^k[n]$ 
11:      return 0
12:    end if
13:  end if
14: end for
15:  $r^3 = \left[ 1 - \exp\left(-\delta \frac{\min_{l \in Y[n]} q_2^l[n]}{u_2^q[n]}\right) \right]$ 
16: return  $\frac{1}{R} (\alpha r^1 + \beta r^2) r^3$ 

```

an RB (W), at an ambient temperature of 300 K. Each UE's receiver is assumed to have a noise figure of 9 dB.

As discussed in Section II, each UE returns a function of its estimated SINR, called the CQI, to the BS. In LTE, CQI is a 4-bit integer. As the relation between CQI and SINR is vendor-specific, we use a simple lookup table to map the estimated SINR to CQI and spectral efficiency. The mapping is given in [26].

As explained in Section II, resource allocation is performed on an RB basis. Each RB is assumed to have a time-width of $T = 1$ ms and a frequency-width of $W = 180$ KHz¹². The number of available RBs at the BS is assumed to be $R = 6$.

¹²These values are set to be the same as those of the LTE standard, which are 180 KHz for bandwidth and 1 ms for time-width of a single resource block [4, 27].

Algorithm 2 Resource allocation algorithm

- 1: Initialize main neural network weights \mathbf{w}^0 and target neural network weights $\mathbf{w}^- = \mathbf{w}^0$.
 - 2: Initialize state $\mathbf{s}_0 \in \mathcal{S}$ and random action $a_0 \in \mathcal{A}$
 - 3: **for** $e = 1, 2, \dots, E$ **do** E : number of episodes
 - 4: **for** $i = 1, 2, \dots, I$ **do** I : number of steps per episode
 - 5: sample a point p from Uniform $[0, 1]$
 - 6: **if** $p < \epsilon$ **then**
 - 7: choose a random action a_i uniformly from \mathcal{A}
 - 8: **else**
 - 9: choose the action as $a_i = \arg \max_a Q(\mathbf{s}_i, a, \mathbf{w})$, where $Q(\mathbf{s}_i, a, \mathbf{w})$ is the output of the neural network
 - 10: **end if**
 - 11: take the action a_i , receive the reward r_i according to Alg. 1, and observe the next state \mathbf{s}_{i+1} from the environment
 - 12: push the tuple $\{\mathbf{s}_i, a_i, r_i, \mathbf{s}_{i+1}, \nu_i\}$ into the replay memory
 - 13: **if** replay memory has enough elements **then**
 - 14: sample a minibatch of size M as $\{\mathbf{s}_j, a_j, r_j, \mathbf{s}_{j+1}, \nu_j\}_{j=1}^M$ from the replay memory
 - 15: set the target for every sample of the minibatch according to (14) as follows
 - 16: **if** $\nu_j == \text{False}$ **then**
 - 17: $y_j = r_j + \gamma \max_a \hat{Q}(\mathbf{s}_{j+1}, a, \mathbf{w}^-)$
 - 18: **else**
 - 19: $y_j = r_j$
 - 20: **end if**
 - 21: update the *main* network weights \mathbf{w} by performing a gradient descent on $\sum_j \|y_j - Q(\mathbf{s}_j, a_j, \mathbf{w})\|^2$
 - 22: update the *target* network weights $\hat{\mathbf{w}}$ once every N_t iterations as $\hat{\mathbf{w}} \leftarrow \mathbf{w}$
 - 23: **end if**
 - 24: **end for**
 - 25: **end for**
-

TABLE I
CHANNEL MODEL PARAMETERS

Parameter	Value	description
$l^j [dB]$	$K - 10\eta \log_{10}(\frac{d^j}{d_0}) + X^j$	large scale fading coefficient between the j th user and the BS
$d^j [m]$	Uniform (10, 100)	distance between i th user and the BS
X^j	$\mathcal{N}(0, \sigma_{sh}^2)$	shadowing effect
σ_{sh}	5.2	shadowing standard deviation
K	$20 \log_{10} \frac{c}{4\pi d_0 f_c}$	free space path loss
$d_0 [m]$	10	reference distance
f_c [GHz]	1	carrier frequency
η	3.5	path loss exponent
ω	0.001	small scale fading correlation parameter

B. Request Generation

For the purpose of simulation, we assume that the arrival process of the requests is Poisson and hence, the inter-arrival time of every two consecutive requests is exponential [28]. Three different service types are considered according to Table II¹³. Each service type has a specific Protocol Data Unit (PDU) size, a maximum tolerable latency and also a specific frequency of generation. The last two columns specify the mean of the inter-arrival times for the requests of each service type. The higher the mean of a request type, the less that type is received by the BS. So, type 1 has the highest frequency of generation and type 3 has the lowest. The length of

¹³Parameters for type 1 and type 2 services are chosen as to correspond to typical real-time audio and video applications, respectively. Type 3 corresponds to more delay-tolerant applications with larger PDUs such as video streaming.

TABLE II
REQUESTS' DISTRIBUTIONS PARAMETERS

service type	PDU size [Kbits]	maximum tolerable latency [ms]	mean of the inter-arrival time [ms]	
			low rate	high rate
type 1	3.2	150	10	5
type 2	64	200	50	25
type 3	200	300	100	50

the BS's requests' buffer is set to $L = 10$, unless otherwise stated.

C. Parameters of the Neural Network

Fully connected layers were used to build the neural network used in the simulations. The detailed parameters are given in Table III.

D. RL Parameters

In order to train the neural network, several episodes are used where in each, a fixed number of RL steps are considered. For each episode, a set of requests are sampled according to the distribution explained in Section VI-B. The number of episodes and the number of RL steps in each episode are given in Table III. The value of $\epsilon[i]$ for each RL step i , used in the ϵ -greedy strategy explained in Section IV-E, is determined based on the following expression [29]

$$\epsilon[i] = \epsilon[i - 1] - \frac{\epsilon_0 - \epsilon_\infty}{\rho}, \quad \forall i \geq 0 \quad (16)$$

where the parameters ϵ_0 , ϵ_∞ , and ρ are given in Table III.

In order to fairly evaluate the proposed scheme against other methods, we consider two sets of iterations of the same size. The agent is mostly trained during the first set, as $\epsilon[i]$ approaches ϵ_∞ by the end of the first set. During the second set, the evaluation parameters are gathered while $\epsilon[i]$ remains equal to ϵ_∞ . As $\epsilon_\infty \neq 0$, the agent is still able to learn during the second set, but the exploration is marginal. Unless otherwise stated, for each set, the number of episodes and the number of RL steps per episode are chosen based on Table III.

E. Evaluation Metrics

In order to measure the capability of the proposed scheme in serving both the licensed and the unlicensed users simultaneously, the following scenario is considered. For the licensed users, the BS receives the requests through a process that was detailed in Section II. At the same time, unlicensed users try to use the spectrum vacancies to communicate. This has the benefit of increasing the overall spectral efficiency of the system, provided that the licensed users' performance is not degraded. As sensing the channel to find vacancies has some overhead, such as the mechanisms used in channel access like CSMA/CA [30], unlicensed users are only able to effectively use the vacancies if the continuity of the vacancy at the same RB exceeds some value (refer to Definition 4).

For unlicensed users, unlike the licensed ones, we do not consider a QoS-aware scheme, as detailed in previous sections. We only consider a single link consisting of a single transmitter and a single receiver. The link channel parameters are exactly the same as those of any of the links between the BS and any licensed user. In summary, for each coherence period, the receiver is put at a random distance to the transmitter with the channel parameters given in Table I and Section II-A. The spectral efficiency for the unlicensed users becomes nonzero as soon as the continuity function, Definition 5, is equal to 1. This can be calculated as

$$\text{SE}_{\text{unlicensed}} = \frac{b_T}{WTN_{\text{unlicensed}}}, \quad (17)$$

where b_T denotes the total number of bits delivered on the unlicensed link and $N_{\text{unlicensed}}$ denotes the total number of unallocated RBs that satisfy the continuity function's constraint, i.e. produce $g_C^k[n] = 1$.

Inspired by (11), we use two different notations to evaluate spectral efficiency for the licensed users, namely $\text{SE}_{\text{licensed}}$ and $\widetilde{\text{SE}}_{\text{licensed}}$, where the former refers to the average spectral efficiency including the allocated bits for the missed requests while in the latter those bits are removed.

The performance of the proposed scheme is measured against that of the two scheduling methods, namely Maximum Throughput (MT) and minimum Latency (mL). The former allocates each RB to the request whose user has the highest spectral efficiency, i.e. $\hat{a}_i = \arg \max_{a_i} \text{SE}(\mathbf{s}_i, a_i)$, and the latter chooses the request with the least normalized TTL, i.e. $\hat{a}_i = \arg \min_{l \in Y[i]} \left(\frac{q_2^l[i]}{u_2^l[i]} \right)$. As these two methods have no control over the continuity of unallocated resources, we give a fraction of the whole bandwidth, in terms of the number of total RBs, to the licensed users and the rest to unlicensed users to be able to compare them with the proposed scheme. We call these two schemes 'MT+F' and 'mL+F', respectively.

Finally, we define the *acceptance ratio* as the ratio of the number of accepted requests, not dropped, to the total number of arrived requests and *missed ratio* as the ratio of the number of missed requests to the number of accepted requests.

F. Numerical Results

The numerical results for the proposed deep RL based algorithm are given in this section. First, we present the learning trend of the proposed scheme in terms of $\text{SE}_{\text{licensed}}$ vs. time steps per episodes against that of a random resource allocation scheme and also of the MT in Fig. 3, where we used 30 episodes for the simulations in total. For the proposed scheme, the parameters

TABLE III
NEURAL NETWORK AND RL PARAMETERS

parameter	value	parameter	value
layers' type	Fully Connected	time steps per episode (I)	500
number of input nodes	$(R+3)L+R+1=97$	replay memory size	100000
number of output nodes	$L+1=11$	minimum number of observations before training	1000
number of hidden layers	3	minibatch size (M)	32
number of nodes for hidden layers	[512, 512, 512]	target network update frequency (in RL steps) (N_t)	100
weight initialization	$\mathcal{N}(0, 0.05)$	ϵ_0	1
learning rate (κ)	0.0001	ϵ_∞	0.01
number of episodes (E)	133	ρ	80000

are chosen as $\alpha = 1$, $\beta = 0$, and $\delta = \infty$. This removes the second and third terms in (11). In other words, the continuity of the unallocated resources and also the latency constraint are both ignored. This makes MT to have the optimum performance in terms of average spectral efficiency. It can be seen that the proposed RL algorithm starts with a performance similar to that of the random assignment scheme and gradually improves as time steps pass and finally achieves the performance of MT. For the results in Fig. 3, 30 episodes are taken and the requests are generated according to the ‘high rate’ column in Table II.

A comparison between the performance of the proposed method and that of the ‘MT+F’ and ‘mL+F’ methods are depicted in Fig. 4 versus the continuity length as in Definition 5. It is seen that the proposed method achieves higher average spectral efficiency (both for the licensed and the unlicensed users) than the other two methods, up to a continuity value of 10 for low arrival rates. It is also seen that increasing the arrival rate (from low to high) causes the proposed method to focus more on the licensed users and hence, $SE_{\text{unlicensed}}$ decreases accordingly. This is in spite of the fact that we increased β and decreased α to strengthen the continuity term in the rewarding mechanism and in turn to maintain $SE_{\text{unlicensed}}$ in part. We can increase β and decrease α even further, but this can cause further reduction in $\widetilde{SE}_{\text{licensed}}$ as well. The proposed method is able to support the uninterrupted communication of the unlicensed users as long as the QoS of the licensed users are guaranteed. When the traffic of the requests is higher, i.e. in high arrival rates, there is less available free resources. As a result, $SE_{\text{unlicensed}}$ drops. The number of RBs given to ‘MT+F’ and ‘mL+F’ are chosen in their favor such that the best sum spectral efficiency

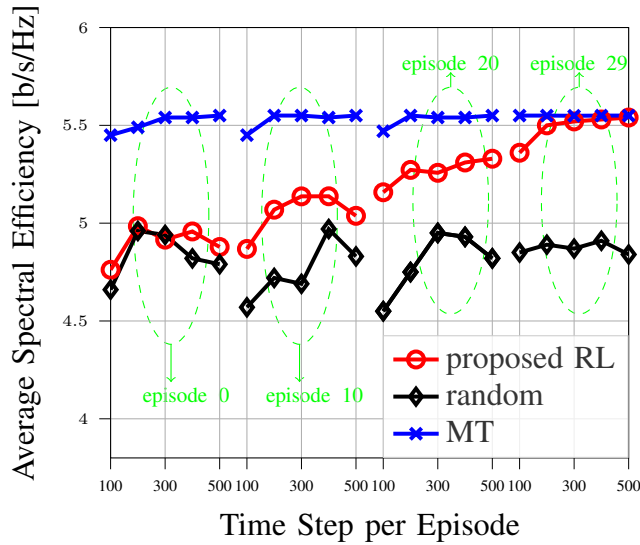


Fig. 3. performance of three different algorithms, namely the ‘proposed deep RL algorithm’, ‘random resource assignment’ and ‘MT’ in terms of average spectral efficiency (over a window of size 1000 RL steps) vs. time steps per episode $\{100, 200, 300, 400, 500\}$ for episodes $\{0, 10, 20, 29\}$. For the proposed scheme the parameters are chosen as $\alpha = 1$, $\beta = 0$, and $\delta = \infty$.

$(\widetilde{SE}_{\text{licensed}} + SE_{\text{unlicensed}})$ is achieved. It is worthwhile to note that ‘mL+F’ can only achieve an acceptance ratio of 88% in high arrival rate with $L = 40$. A more fair comparison would be to consider it with $L = 50$ against the other two methods with $L = 40$. This decreases the sum spectral efficiency of ‘mL+F’ to 4.24 b/s/Hz which is less than that of the proposed method.

In Fig. 5, the CDF of the delivered/missed PDUs of the requests for the proposed method is depicted against that of the ‘MT+F’ and ‘mL+F’ methods. It is seen that the proposed method serves all three types of requests well before their deadlines. In fact it acts, in terms of latency, similar to ‘mL’, as it takes into account the maximum tolerable latencies of the requests. ‘MT+F’ method, however, missed many of the requests of type 3 as it only takes into account the instantaneous spectral efficiency. The missed ratio shows that the proposed method delivers the requests with $2e-4$ missed ratio, while ‘MT+F’ has a missed ratio of $5e-2$.

The performance of the three methods vs. the buffer length (L) in terms of missed ratio and acceptance ratio are depicted in Fig. 6. It is seen that the proposed method can achieve up to 99.6% acceptance ratio for high arrival rate by increasing buffer length from 10 to 50. It is also seen that the proposed method has the least increase in missed ratio by increasing the buffer length among the three methods and can also accept almost all of the incoming requests with

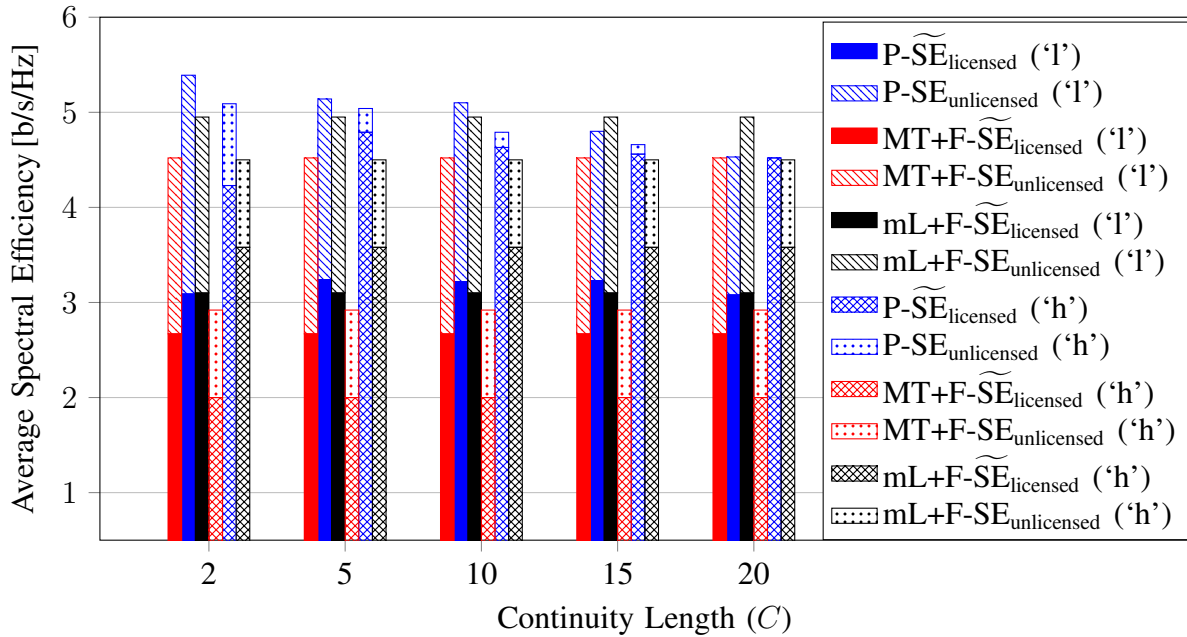


Fig. 4. Average spectral efficiency ($\widetilde{SE}_{\text{licensed}}$, $SE_{\text{unlicensed}}$) for the proposed method ('P') against that of the 'MT+F' and 'mL+F' methods versus the continuity length (C) (Definition 5) for two different arrival rates (for all cases $L = 40$): Low ('l'), where $\alpha = 2, \beta = 2, \delta = 1$ for the proposed method. For 'MT+F' and 'mL+F', 4 RBs are given to the licensed and 2 RBs given to the unlicensed users. High ('h'), where $\alpha = 1.5, \beta = 2.5, \delta = 1$ for the proposed method. For 'MT+F' and 'mL+F', 5 RBs are given to the licensed and 1 RB is given to the unlicensed users. The missed ratio for 'MT+F' and 'mL+F' methods are 0.15 and 0.1, respectively while at most 0.08 for the proposed method.

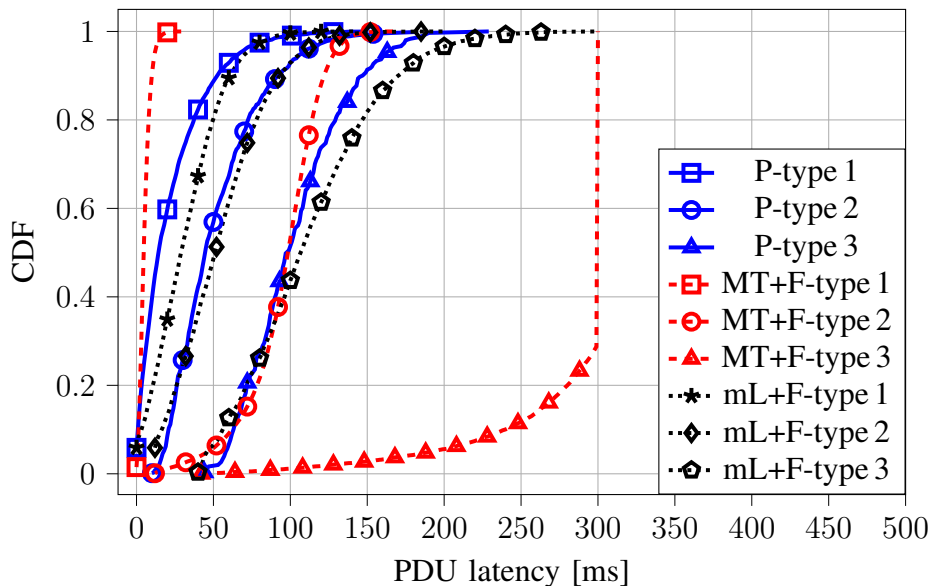


Fig. 5. CDF of the aggregated latency of the delivered and missed PDUs for the proposed method ('P') (with $\alpha = \beta = 2, \delta = 1$, $C = 2$) against that of the 'MT+F' and 'mL+F' methods for different service types in high arrival rate (for all cases $L = 10$). The missed ratio for 'P', 'MT+F' and 'mL+F' methods are $\{2e-4, 5e-2, 2.5e-5\}$, respectively.

the least missed ratio among all the methods.

$\widetilde{SE}_{\text{licensed}}$ and $SE_{\text{unlicensed}}$ are also compared in Fig. 7 for low and high arrival rates in terms of buffer length. All the three methods show slight variation, in terms of spectral efficiency, for low arrival rates. This is due to the fact that the buffer with $L = 10$ almost suffices to hold all the incoming requests. For high arrival rates, however, spectral efficiencies change with the change of buffer length. As the buffer length increases, more requests are accepted and should be handled in time. The proposed method, as noted earlier, can handle almost all of the requests with the least decrease in sum spectral efficiency. The other two methods fall short in serving all of the incoming requests.

VII. ACKNOWLEDGMENT

The work by Mahdi Nouri Boroujerdi is supported by Iran National Science Foundation (INSF). The work by Babak Hossein Khalaj, Mohammad Ali Maddah-Ali, Mohammad Akbari and Roghayeh Joda is funded by ICT Research Institute (ITRC).

VIII. CONCLUSION

In this paper, we proposed a deep-RL-based resource allocation for a cellular network which can make a balance among spectral efficiency, from the network manager perspective, the quality of service, from the users' perspective, and smoothness of the unallocated resources, which is beneficial to the unlicensed users. Results show that the proposed scheme can efficiently make such balance through the proposed learning mechanism.

REFERENCES

- [1] W. S. H. M. W. Ahmad, N. A. M. Radzi, F. S. Samidi, A. Ismail, F. Abdullah, M. Z. Jamaludin, and M. N. Zakaria, "5G technology: Towards dynamic spectrum sharing using cognitive radio networks," *IEEE Access*, vol. 8, pp. 14460–14488, 2020.
- [2] B. Bojovi, L. Giupponi, Z. Ali, and M. Miozzo, "Evaluating unlicensed LTE technologies: LAA vs LTE-U," *IEEE Access*, vol. 7, pp. 89714–89751, 2019.
- [3] Q. Yang, Y. Huang, Y. Yen, L. Chen, H. Chen, X. Hong, J. Shi, and L. Wang, "Location based joint spectrum sensing and radio resource allocation in cognitive radio enabled LTE-U systems," *IEEE Transactions on Vehicular Technology*, vol. 69, no. 3, pp. 2967–2979, 2020.
- [4] F. Capozzi, G. Piro, L. A. Grieco, G. Boggia, and P. Camarda, "Downlink packet scheduling in LTE cellular networks: Key design issues and a survey," *IEEE Communications Surveys Tutorials*, vol. 15, no. 2, pp. 678–700, 2013.

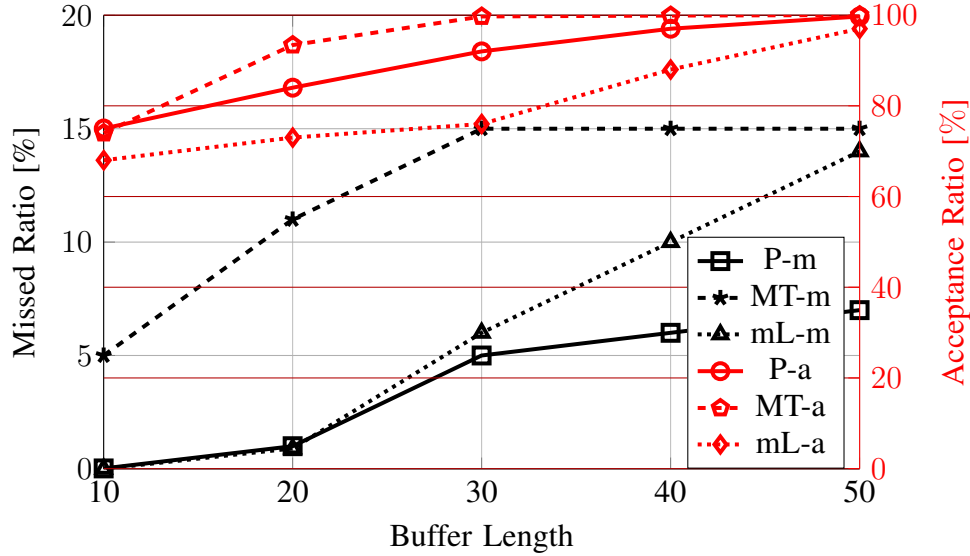


Fig. 6. Missed ratio ('m') on the left axis and acceptance ratio ('a') on the right axis for the proposed method ('P') (with $\alpha = \beta = 2, \delta = 1, C = 2$) against those of the 'MT+F' and 'mL+F' methods versus buffer length (L) in high arrival rate (for all cases $L = 10$).

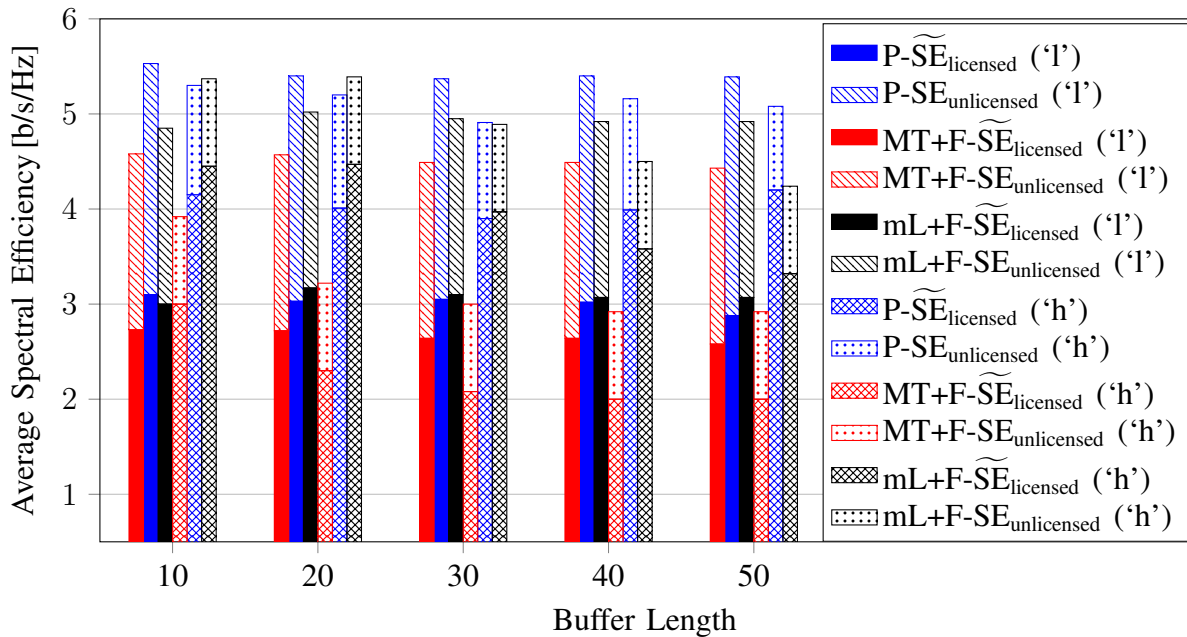


Fig. 7. Average spectral efficiency ($\widetilde{SE}_{\text{licensed}}, SE_{\text{unlicensed}}$) for the proposed method ('P') against that of the 'MT+F' and 'mL+F' methods versus buffer length (L) with $C = 2$ (Definition 5) for two different arrival rates: Low ('l'), where $\alpha = 2, \beta = 2, \delta = 1$ for the proposed method. For 'MT+F' and 'mL+F', 4 RBs are given to the licensed and 2 RBs given to the unlicensed users. High ('h'), where $\alpha = 1.5, \beta = 2.5, \delta = 1$ for the proposed method. For 'MT+F' and 'mL+F', 5 RBs are given to the licensed and 1 RB is given to the unlicensed users.

- [5] J. Tan, S. Xiao, S. Han, Y. Liang, and V. C. M. Leung, "Qos-aware user association and resource allocation in LAA-LTE/WiFi coexistence systems," *IEEE Transactions on Wireless Communications*, vol. 18, no. 4, pp. 2415–2430, April 2019.
- [6] Y. L. Lee, J. Loo, T. C. Chuah, and A. A. El-Saleh, "Fair resource allocation with interference mitigation and resource reuse for LTE/LTE-A femtocell networks," *IEEE Transactions on Vehicular Technology*, vol. 65, no. 10, pp. 8203–8217, 2016.
- [7] C. Jiang, H. Zhang, Y. Ren, Z. Han, K. Chen, and L. Hanzo, "Machine learning paradigms for next-generation wireless networks," *IEEE Wireless Communications*, vol. 24, no. 2, pp. 98–105, April 2017.
- [8] Q. Mao, F. Hu, and Q. Hao, "Deep learning for intelligent wireless networks: A comprehensive survey," *IEEE Communications Surveys Tutorials*, vol. 20, no. 4, pp. 2595–2621, Fourthquarter 2018.
- [9] N. C. Luong, D. T. Hoang, S. Gong, D. Niyato, P. Wang, Y. Liang, and D. I. Kim, "Applications of deep reinforcement learning in communications and networking: A survey," *IEEE Communications Surveys Tutorials*, vol. 21, no. 4, pp. 3133–3174, Fourthquarter 2019.
- [10] E. C. Santos, "A simple reinforcement learning mechanism for resource allocation in LTE-A networks with Markov decision process and Q-learning," *CoRR*, vol. abs/1709.09312, 2017. [Online]. Available: <http://arxiv.org/abs/1709.09312>
- [11] V. Mnih, K. Kavukcuoglu, D. Silver, A. A. Rusu, J. Veness, M. G. Bellemare, A. Graves, M. Riedmiller, A. K. Fidjeland, G. Ostrovski, S. Petersen, C. Beattie, A. Sadik, I. Antonoglou, H. King, D. Kumaran, D. Wierstra, S. Legg, and D. Hassabis, "Human-level control through deep reinforcement learning," *Nature*, vol. 518, no. 7540, pp. 529–533, 2015. [Online]. Available: <https://doi.org/10.1038/nature14236>
- [12] R. Li, Z. Zhao, Q. Sun, C. I, C. Yang, X. Chen, M. Zhao, and H. Zhang, "Deep reinforcement learning for resource management in network slicing," *IEEE Access*, vol. 6, pp. 74429–74441, 2018.
- [13] N. Zhao, Y. Liang, D. Niyato, Y. Pei, M. Wu, and Y. Jiang, "Deep reinforcement learning for user association and resource allocation in heterogeneous cellular networks," *IEEE Transactions on Wireless Communications*, vol. 18, no. 11, pp. 5141–5152, Nov 2019.
- [14] U. Challita, L. Dong, and W. Saad, "Proactive resource management for LTE in unlicensed spectrum: A deep learning perspective," *IEEE Transactions on Wireless Communications*, vol. 17, no. 7, pp. 4674–4689, July 2018.
- [15] W. Zhang, C. Wang, X. Ge, and Y. Chen, "Enhanced 5G cognitive radio networks based on spectrum sharing and spectrum aggregation," *IEEE Transactions on Communications*, vol. 66, no. 12, pp. 6304–6316, 2018.
- [16] "5G; NR; Physical layer procedures for data," ETSI, Tech. Rep. ETSI TS 138 214, 2019.
- [17] S. Sesia, I. Toufik, and M. Baker, *LTE, The UMTS Long Term Evolution: From Theory to Practice*. Wiley Publishing, 2009.
- [18] R. S. Sutton and A. G. Barto, *Reinforcement Learning: An Introduction*, 2nd ed. Cambridge, MA, USA: The MIT Press, 2020.
- [19] C. Szepesvári, *Algorithms for Reinforcement Learning*, ser. Synthesis lectures on artificial

- intelligence and machine learning. Morgan & Claypool, 2010. [Online]. Available: <https://books.google.com/books?id=qwtphf7U74C>
- [20] B. C. Csáji, “Approximation with artificial neural networks,” Master’s thesis, Faculty of Sciences, Eötvös Loránd University, Hungary, 2001.
- [21] Z. Lu, H. Pu, F. Wang, Z. Hu, and L. Wang, “The expressive power of neural networks: A view from the width,” in *Advances in Neural Information Processing Systems* 30, I. Guyon, U. V. Luxburg, S. Bengio, H. Wallach, R. Fergus, S. Vishwanathan, and R. Garnett, Eds. Curran Associates, Inc., 2017, pp. 6231–6239. [Online]. Available: <http://papers.nips.cc/paper/7203-the-expressive-power-of-neural-networks-a-view-from-the-width.pdf>
- [22] V. Mnih, K. Kavukcuoglu, D. Silver, A. A. Rusu, J. Veness, M. G. Bellemare, A. Graves, M. Riedmiller, A. K. Fidjeland, G. Ostrovski, S. Petersen, C. Beattie, A. Sadik, I. Antonoglou, H. King, D. Kumaran, D. Wierstra, S. Legg, and D. Hassabis, “Human-level control through deep reinforcement learning,” *Nature*, vol. 518, no. 7540, pp. 529–533, Feb. 2015. [Online]. Available: <http://dx.doi.org/10.1038/nature14236>
- [23] A. Goldsmith, *Wireless Communications*, 1st ed. Cambridge University Press, 2005.
- [24] S. Chou, T. Chiu, Y. Yu, and A. Pang, “Mobile small cell deployment for next generation cellular networks,” in *2014 IEEE Global Communications Conference*, 2014, pp. 4852–4857.
- [25] T. S. Rappaport, *Wireless Communications: Principles and Practice*, 2nd ed. Prentice Hall, 2002.
- [26] H. Zarrinkoub, *Understanding LTE with MATLAB: From Mathematical Modeling to Simulation and Prototyping*. Wiley Publishing, 01 2013.
- [27] Y. L. Lee, T. C. Chuah, J. Loo, and A. Vinel, “Recent advances in radio resource management for heterogeneous LTE/LTE-A networks,” *IEEE Communications Surveys Tutorials*, vol. 16, no. 4, pp. 2142–2180, Fourthquarter 2014.
- [28] A. Papoulis and S. U. Pillai, *Probability, Random Variables, and Stochastic Processes*, 4th ed. Boston: McGraw Hill, 2002.
- [29] M. Tokic and G. Palm, “Value-difference based exploration: Adaptive control between epsilon-greedy and softmax,” in *KI 2011: Advances in Artificial Intelligence*, J. Bach and S. Edelkamp, Eds. Berlin, Heidelberg: Springer Berlin Heidelberg, 2011, pp. 335–346.
- [30] D. E. Comer, *Computer Networks and Internets*, 6th ed. Pearson, 2014.